Analytical Biochemistry 483 (2015) 34–39

Contents lists available at ScienceDirect

Analytical Biochemistry

journal homepage: www.elsevier.com/locate/yabio

A continuous spectrophotometric assay for monitoring adenosine 5′-monophosphate production

Eric A. First *

Department of Biochemistry and Molecular Biology, Louisiana State University Health Sciences Center in Shreveport, Shreveport, LA 71130, USA

ARTICLE INFO

Article history:
Received 22 December 2014
Received in revised form 24 April 2015
Accepted 27 April 2015
Available online 6 May 2015

Keywords:
AMP
High-throughput assay
AMP deaminase
IMP dehydrogenase
Aminoacyl–tRNA synthetase
cAMP phosphodiesterase

ABSTRACT

A number of biologically important enzymes release adenosine 5′-monophosphate (AMP) as a product, including aminoacyl–tRNA synthetases, cyclic AMP (cAMP) phosphodiesterases, ubiquitin and ubiquitin-like ligases, DNA ligases, coenzyme A (CoA) ligases, polyA deadenylases, and ribonucleases. In contrast to the abundance of assays available for monitoring the conversion of adenosine 5′-triphosphate (ATP) to ADP, there are relatively few assays for monitoring the conversion of ATP (or cAMP) to AMP. In this article, we describe a homogeneous assay that continuously monitors the production of AMP. Specifically, we have coupled the conversion of AMP to inosine 5′-monophosphate (IMP) (by AMP deaminase) to the oxidation of IMP (by IMP dehydrogenase). This results in the reduction of oxidized nicotine adenine dinucleotide (NAD^+) to reduced nicotine adenine dinucleotide (NADH), allowing AMP formation to be monitored by the change in the absorbance at 340 nm. Changes in AMP concentrations of 5 μM or more can be reliably detected. The ease of use and relatively low expense make the AMP assay suitable for both high-throughput screening and kinetic analyses.

© 2015 Elsevier Inc. All rights reserved.

High-throughput screening assays are a staple of drug discovery, allowing more than 100,000 compounds to be screened per day [1]. Targets of high-throughput screens include G-protein-coupled receptors, enzymes, hormones, ion channels, nuclear receptors, and DNA transcription factors. In addition to identifying lead compounds (“hits”), drug development requires high-throughput assays to eliminate false positives, validate the target, prioritize the hits, and elucidate structure–activity relationships. The development of high-throughput assays is also required to keep pace with the rapid growth of genomic and proteomic data. With this in mind, we have developed a homogeneous, continuous spectrophotometric assay for monitoring the production of adenosine 5′-monophosphate (AMP).[1]

A number of enzymes release AMP as a product, including aminoacyl–tRNA synthetases, cyclic AMP (cAMP) phosphodiesterases, ubiquitin and ubiquitin-like ligases, DNA ligases, coenzyme A (CoA) ligases, polyA deadenylases, and ribonucleases. Many of these enzymes are either current or potential drug targets for a wide range of diseases and disorders. The assay described in this article consists of two steps: (i) deamination of AMP to produce inosine 5′-monophosphate (IMP) and (ii) the oxidation of IMP by oxidized nicotine adenine dinucleotide (NAD^+) to produce xanthine 5′-monophosphate (XMP) and reduced nicotine adenine dinucleotide (NADH) (Fig. 1). These reactions are catalyzed by AMP deaminase and IMP dehydrogenase, respectively. Because the production of NADH is accompanied by an increase in absorbance at 340 nm, the release of AMP can be monitored continuously, allowing it to be used for both high-throughput screening and the subsequent kinetic analysis of lead compounds. In this article, we validate the use of this assay for monitoring the production of AMP.

Materials and methods

Materials

Materials were obtained from the following sources: *Saccharomyces cerevisiae* clones containing the open reading frames for AMP deaminase and IMP dehydrogenase (Open Biosystems/GE Healthcare Life Sciences, Lafayette, CO, USA); TOPO TA Cloning Kit (Life Technologies, Grand Island, NY, USA); Wizard SV Gel and PCR Clean-Up System (Promega, Madison, WI, USA); pET30a(+) expression vector and Rosetta 2 DE3 *Escherichia coli* cells (EMD Biosciences, Billerica, MA, USA); XL2 Blue *E. coli* cells

* Fax: +1 318 675 5180.
E-mail address: efirst@lsuhsc.edu

[1] *Abbreviations used:* AMP, adenosine 5′-monophosphate; cAMP, cyclic AMP; CoA, coenzyme A; IMP, inosine 5′-monophosphate; NAD^+, oxidized nicotine adenine dinucleotide; XMP, xanthine 5′-monophosphate; NADH, reduced nicotine adenine dinucleotide; PCR, polymerase chain reaction; PDE, phosphodiesterase.

http://dx.doi.org/10.1016/j.ab.2015.04.032
0003-2697/© 2015 Elsevier Inc. All rights reserved.

(Agilent Technologies, Santa Clara, CA, USA); E.Z.N.A. Plasmid DNA Mini I Kit (Omega Bio-Tek, Norcross, GA, USA); T4 DNA ligase, NcoI-HF, and XhoI (New England Biolabs, Ipswich, MA, USA); Taq DNA polymerase (G-Biosciences, St. Louis, MO, USA); AMP (Research Products International, Mount Prospect, IL, USA); ATP, IMP, and NAD^+ (VWR International, Radnor, PA, USA); and oligonucleotides (Integrated DNA Technologies, Coralville, IA, USA). All other reagents were obtained from ThermoFisher Scientific (Waltham, MA, USA). DNA sequencing was performed by the DNA Lab at Arizona State University. Curve fitting and graphing were performed using GraFit (Erithacus Software, Horley, Surrey, UK) and Kaleidograph (Synergy Software, Reading, PA, USA).

Subcloning AMP deaminase and IMP dehydrogenase into the pET30a(+) expression vector

The polymerase chain reaction (PCR) was used to amplify the open reading frames for *S. cerevisiae* AMP deaminase and IMP dehydrogenase (Open Biosystems clones YML035C and YLR432W, respectively). Primers were designed such that the amplified DNA contained unique NcoI and XhoI sites at the 5′ and 3′ ends, respectively. Amplified open reading frames were initially ligated into the PCR2.1–TOPO TA vector and transformed into XL2 Blue cells. Individual colonies were selected and grown overnight in 2 ml of 2 × YT medium (16 g/L tryptone, 10 g/L yeast extract, and 5 g/L NaCl), followed by PCR screening to identify positive clones. Plasmids were isolated from the positive cultures using an E.Z.N.A. Plasmid DNA Mini I Kit, and the inserted DNA was sequenced by the Arizona State University DNA Sequencing Facility. The open reading frames were subsequently removed by digestion with NcoI–HF and XhoI, gel purified using the Wizard SV Gel and PCR Clean-Up System, and subcloned into the pET30a(+) vector such that subsequent expression results in a protein containing an amino-terminal S-Tag/His-Tag followed by either AMP deaminase or IMP dehydrogenase. The AMP deaminase and IMP dehydrogenase coding sequences in the pET30a(+) vector were sequenced in their entirety. These plasmids are designated pADA1–WT and pIDH1–WT, respectively. All procedures involving recombinant DNA were performed using National Institutes of Health (NIH) biosafety level 1 containment procedures and were approved by the Louisiana State University Health Sciences Center biosafety committee.

Protein expression and purification

AMP deaminase and IMP dehydrogenase were expressed in *E. coli* Rosetta 2 DE3 cells harboring the pADA1–WT and pIDH1–WT plasmids, respectively. Purification of the recombinant proteins was carried out by Ni–NTA affinity chromatography using a procedure analogous to that described previously for the purification of human tyrosyl–tRNA synthetase [2,3]. Proteins were purified to >95% homogeneity based on sodium dodecyl sulfate–polyacrylamide gel electrophoresis (SDS–PAGE). Protein concentrations were calculated based on A_{280} measurements (ε_{280} = 470,320 and 99,480 $M^{-1}\,cm^{-1}$ for the AMP deaminase and IMP dehydrogenase homotetramers, respectively, as determined by the ExPASy ProtParam tool [4]). Purified proteins were stored at −70 °C in buffer containing 50 mM Tris (pH 7.5), 20 mM β-mercaptoethanol, 10 mM $MgCl_2$, and 10% (v/v) glycerol.

Kinetic analyses

IMP dehydrogenase was assayed in buffer containing 50 mM Tris (pH 7.2), 100 mM KCl, 0.1 mM dithiothreitol, and either 5 mM IMP or 5 mM NAD^+ (for determination of K_m^{NAD+} and K_m^{IMP}, respectively). To determine the K_m^{NAD+} and K_m^{IMP} values, the concentrations of NAD^+ and IMP were varied from 0 to 5 mM and the conversion of NAD^+ to NADH was monitored at 340 nm (ε_{340} = 6220 $M^{-1}\,cm^{-1}$). AMP deaminase was assayed in buffer containing 50 mM Tris (pH 7.2), 100 mM KCl, 2 mM ATP, 8 mM $MgCl_2$, 0.1 mM dithiothreitol, 5 mM NAD^+, and 3 μM IMP dehydrogenase. To determine K_m^{AMP}, the concentration of AMP was varied from 0 to 5 mM and the conversion of NAD^+ to NADH was monitored as described above. The pH of all stock solutions (e.g., IMP, NAD^+, ATP, AMP) was adjusted to 7.0 prior to use. All kinetic assays were performed in 96-well microtiter plates at 25 °C using 200 μl of assay mix per well. Under these conditions, the path length is 0.56 cm. All assays were monitored by following the change in absorbance at 340 nm over 10 min using a Synergy 4 Hybrid Microplate Reader (BioTek, Winooski, VT, USA).

The pH profile for IMP dehydrogenase was determined by assaying the enzyme in the presence of 100 mM KCl, 0.1 mM dithiothreitol, 5 mM IMP, 5 mM NAD^+, and 50 mM of either sodium phosphate (pH 5.5–7.5) or Tris (pH 7.5–9.0). The pH profile for AMP deaminase was determined by assaying the enzyme in the presence of 100 mM KCl, 0.1 mM dithiothreitol, 5 mM AMP, 2 mM ATP, 8 mM $MgCl_2$, 1.5 μM IMP dehydrogenase, and 50 mM of either sodium phosphate (pH 5.5–7.5) or Tris (pH 7.5–9.0).

Initial rates for each substrate concentration were determined from a linear fit of the data (A_{340} vs. time). K_m and V_{max} values were determined by fitting a plot of initial rate versus substrate concentration to the Michaelis–Menten equation [5,6]:

$$v_o = \frac{V_{max}[S]}{K_m + [S]}, \tag{1}$$

where v_o is the initial rate of the reaction and [S] is the substrate concentration. The k_{cat} values were calculated from the following equation [5,6]:

$$V_{max} = k_{cat}[E], \tag{2}$$

where [E] is the molar concentration of the enzyme in the assay.

Results

Determination of K_m and k_{cat} values for IMP dehydrogenase

IMP dehydrogenase catalyzes the first committed step in guanine biosynthesis, the oxidation of IMP by NAD^+ (Fig. 1). This reaction can be monitored by the increase in absorbance at 340 nm resulting from the production of NADH. Because the oxidation of IMP will be coupled to the AMP deaminase-catalyzed conversion of AMP to IMP, kinetic parameters for the reaction were determined at pH 7.2. As shown in Fig. 2, IMP dehydrogenase from *S. cerevisiae* follows classical Michaelis–Menten kinetics with respect to both the IMP and NAD^+ substrates. Although the steady-state kinetic parameters for *S. cerevisiae* IMP dehydrogenase have not been published previously, comparison with the k_{cat} and K_m values for *Candida albicans* IMP dehydrogenase indicates that the k_{cat} value is similar for the two IMP dehydrogenase homologs [7]. In contrast, *S. cerevisiae* IMP dehydrogenase binds IMP with a 7-fold lower affinity and binds NAD^+ with a 4-fold higher affinity than the *C. albicans* homolog (Table 1).

Determination of K_m and k_{cat} values for AMP deaminase

AMP deaminase catalyzes the deamination of AMP, forming IMP and NH_4^+ (Fig. 1). This reaction is the first step in the purine nucleotide cycle, which ultimately results in the production of fumarate from aspartic acid. Both ATP and MgATP have been reported to allosterically activate *S. cerevisiae* AMP deaminase [8–10]. To ensure that AMP deaminase is the limiting enzyme in the assay,

Fig.1. Reaction scheme coupling AMP to the production of NADH. AMP deaminase and IMP dehydrogenase are used to couple the production of AMP to the reduction of NAD^+. AMP production is monitored by following the increase in absorbance at 340 nm that occurs as a result of the reduction of NAD^+ to NADH.

varying ratios of AMP deaminase/IMP dehydrogenase were assayed. AMP deaminase/IMP dehydrogenase molar ratios of 1:15 or less were found to result in a linear dependence on AMP deaminase (data not shown). Subsequent kinetic measurements were performed using ratios of AMP deaminase/IMP dehydrogenase at or below this threshold. In agreement with previous investigators, we found that in the presence of ATP, AMP deaminase from *S. cerevisiae* follows classical Michaelis–Menten kinetics (Fig. 3) [8,9]. The K_m^{AMP} value for *S. cerevisiae* AMP deaminase is within experimental error of previously reported values (Table 1). In contrast, the k_{cat} value for the recombinant *S. cerevisiae* AMP deaminase is 200-fold less than previously reported values for AMP deaminase purified from Baker's yeast (Table 1). The reason for the lower k_{cat} value of the recombinant enzyme remains to be determined. It is possible that the amino-terminal S-tag/His-tag inhibits the activity of the recombinant AMP deaminase. The presence or absence of bovine serum albumin (0.5 mg/ml) had no significant effect on either K_m^{AMP} or k_{cat} of the *S. cerevisiae* AMP deaminase (data not shown).

Determination of optimal pH for coupled assay

To determine the optimal pH for the coupled assay, the pH profiles for IMP dehydrogenase and AMP deaminase were determined between pH 5.5 and 9.0 using 50 mM of either sodium phosphate (pH 5.5–7.5) or Tris (pH 7.5–9.0) as buffers. The AMP deaminase activity was measured using the coupled assay under conditions where it is the rate-limiting enzyme for all pH values. As a result, the pH profile determined for AMP deaminase and the pH profile for the overall coupled reaction are identical.

Although inorganic phosphate has previously been reported to be inhibitory with respect to AMP deaminase [8,9], we observed only minor differences between the sodium phosphate and Tris buffers at pH 7.5. IMP dehydrogenase exhibits a peak of activity at pH 8.5 (Fig. 4A). AMP deaminase displays significant activity between pH 6.5 and 8.5, with maximum activity at pH 7.5 (Fig. 4B).

Discussion

Enzymes that release AMP as a product play a role in a number of diseases. For example, cAMP phosphodiesterases (PDEs) convert cAMP to AMP and, as a result, regulate signal transduction pathways governing vascular resistance, cardiac output, visceral motility, immune response, inflammation, neuroplasticity, vision, and reproduction [11–16]. PDE inhibitors prolong or enhance cAMP-mediated signaling pathways and have been used in the treatment of pulmonary arterial hypertension, coronary heart disease, dementia, depression, schizophrenia, and other disorders [12–16]. Other enzymes that release AMP as a product include the ubiquitin ligase and ubiquitin-like ligase proteins, which catalyze the attachment of ubiquitin and ubiquitin-like proteins (e.g., small ubiquitin-like modifier [SUMO] proteins) to their protein substrates, modifying their function or targeting them for degradation by the proteasome [17–19]. Like proteasome inhibitors, inhibitors of ubiquitin ligases have potential therapeutic value in treating cancer and other diseases by inducing apoptosis

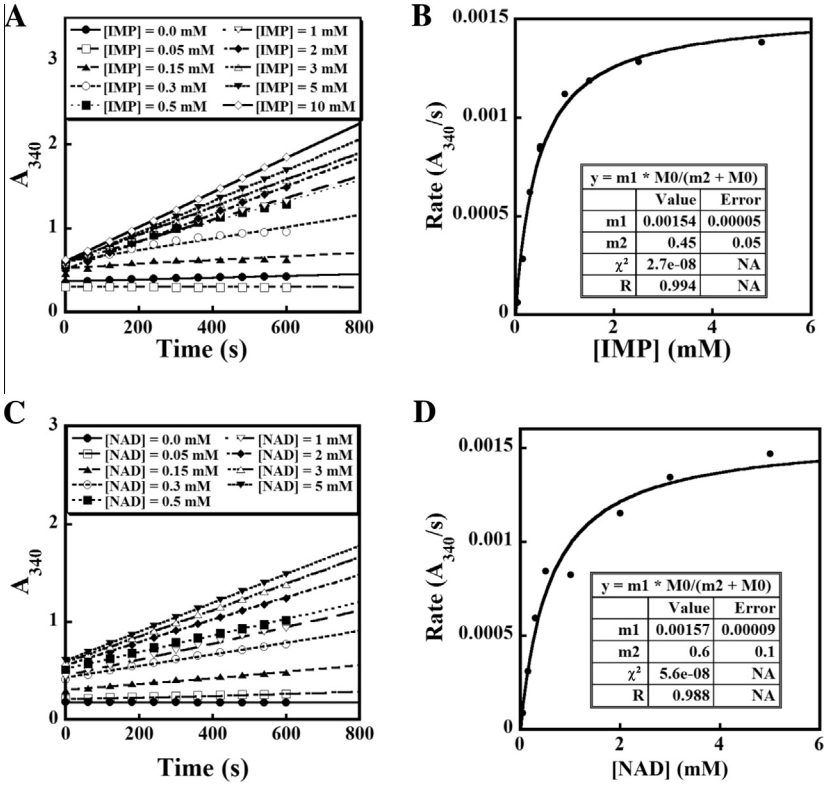

Fig.2. Monitoring IMP dehydrogenase activity by the production of NADH. IMP dehydrogenase activity was monitored by following the increase in absorbance at 340 nm. The concentration of IMP dehydrogenase in the assays is 0.76 μM. (A) Time course assays for IMP dehydrogenase at various concentrations of IMP are shown. (B) A plot of reaction rate versus IMP concentration for IMP dehydrogenase is shown (reaction rates were determined from linear fits of the time course assays shown in panel A). (C) Time course assays for IMP dehydrogenase at various concentrations of NAD^+ are shown. (D) A plot of reaction rate versus NAD^+ concentration for IMP dehydrogenase is shown (reaction rates were determined from linear fits of the time course assays shown in panel C). The data in panels B and D are fit to Eq. (1).

Table 1
Kinetic constants for IMP dehydrogenase and AMP deaminase.

Enzyme	Substrate	K_m (mM)[a]	k_{cat} (s^{-1})[a,b]
IMP dehydrogenase (*S. cerevisiae*)	IMP	0.42 (±0.08)	3.5 (±0.5)
IMP dehydrogenase (*S. cerevisiae*)	NAD^+	0.8 (±0.1)	–
AMP deaminase (*S. cerevisiae*)	AMP	0.4 (±0.1)	21 (±4)
IMP dehydrogenase (*C. albicans*)[c]	IMP	0.06	6
IMP dehydrogenase (*C. albicans*)[c]	NAD^+	3.5	–
AMP deaminase (Brewer's yeast)[d]	AMP	0.2	4500

[a] Standard error values are shown in parentheses. K_m and k_{cat} values are the averages of at least three independent assays using two or more different protein preparations.
[b] The k_{cat} value for IMP dehydrogenase is the average k_{cat} value calculated using both the IMP- and NAD^+-dependent reaction rate data.
[c] The K_m and k_{cat} values are taken from Ref. [7].
[d] The K_m and k_{cat} values are taken from Ref. [8]. The k_{cat} value is calculated from the specific activity.

[20–23]. However, because ubiquitin ligases target specific subsets of proteins for degradation, they are more selective than proteasome inhibitors [24,25]. Enzymes that remove these protein modifications (e.g., deubiquitinating enzymes) also target selected subsets of proteins, providing additional candidates for therapeutic intervention [26]. Lastly, members of the aminoacyl–tRNA synthetase family release AMP as a product during the aminoacylation of tRNA, a crucial step in protein synthesis. Members of this family are potential targets for the development of novel antibiotics and antifungals [27–29]. For example, an isoleucyl–tRNA synthetase inhibitor, mupirocin, is used to treat multidrug-resistant *Staphylococcus aureus*, whereas a leucyl–tRNA synthetase inhibitor, Kerydin, is an antifungal that recently received U.S. Food and Drug Administration (FDA) approval for the topical treatment of onychomycosis of the toenails [30,31]. Furthermore, the essential role that aminoacyl–tRNA synthetases play in protein synthesis makes the human homologs potential targets for chemotherapy agents.

Currently, two assays are commercially available to monitor the production of AMP. The AMP-Glo assay (Promega) relies on the enzymatic conversion of AMP to ATP and the subsequent conversion of D-luciferin and ATP to oxyluciferin by firefly luciferase, producing light at 560 nm [32]. Because the reaction is quenched prior to the conversion of AMP to ATP, individual assays must be performed for each time point. A second commercially available assay, the Transcreener assay (BellBrook Labs, Madison, WI, USA), uses an anti-AMP antibody complexed with a fluorescent tracer [33]. Binding of AMP to the antibody releases the fluorescent tracer, allowing the amount of AMP to be quantified by measuring either the fluorescence polarization of the tracer or time-resolved fluorescence resonance energy transfer between the tracer and antibody.

An alternative to monitoring formation of the AMP product is to monitor formation of the pyrophosphate product that results from cleavage of ATP. This can be done by using inorganic pyrophosphatase to cleave pyrophosphate and determining the amount of phosphate produced. There are several commercially available assays that use this approach. A number of assays use malachite green and ammonium molybdate, which forms a chromogenic complex with inorganic phosphate that absorbs at 630 nm (ε_{630} = 90,000 M^{-1} cm^{-1}) [34,35]. Although this assay is very sensitive, aliquots must be removed and quenched at each time point to determine the production of AMP. This limitation is overcome in the EnzChek assay (Life Technologies), which uses purine nucleoside phosphorylase to convert 2-amino-6-mercapto-7-methylpurine riboside (MESG) and inorganic phosphate to ribose

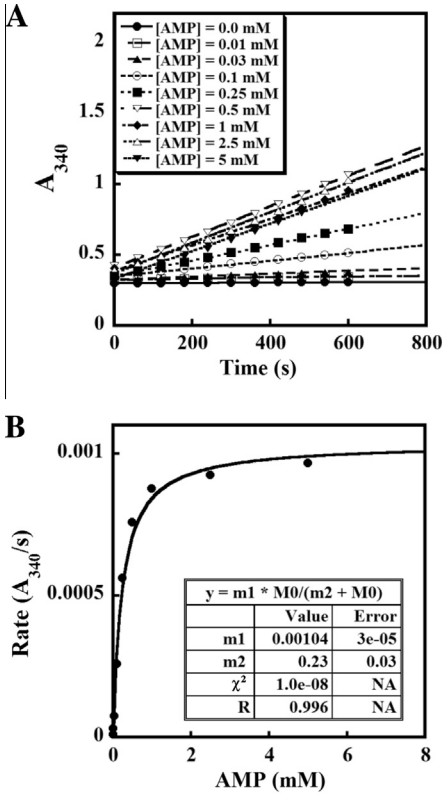

Fig.3. Monitoring AMP deaminase activity by coupling it to the IMP dehydrogenase reaction. AMP deaminase activity was monitored by following the increase in absorbance at 340 nm. The concentrations of IMP dehydrogenase and AMP deaminase in the assays are 3 μM and 0.24 μM, respectively. (A) Time course assays for AMP deaminase at various concentrations of AMP are shown. (B) A plot of reaction rate versus AMP concentration for the AMP deaminase is shown (reaction rates were determined from linear fits of the time course assays shown in panel A). The data in panel B are fit to Eq. (1).

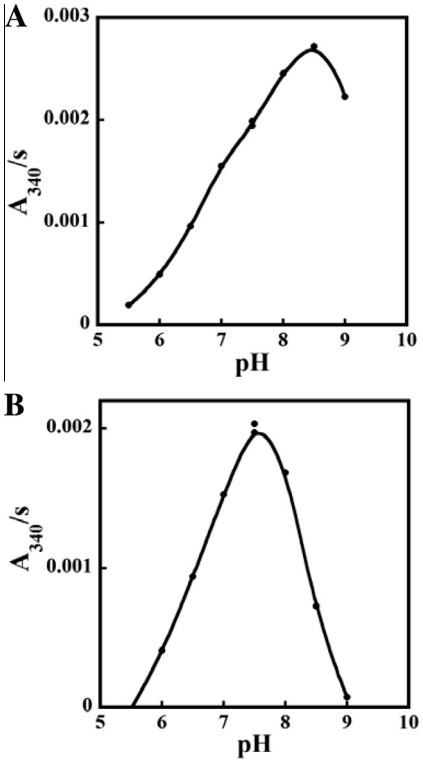

Fig.4. pH profiles for IMP dehydrogenase and AMP deaminase. The pH profiles for IMP dehydrogenase activity (A) and AMP deaminase activity (B) are shown. The pH of the assay was varied by buffering with either 50 mM sodium phosphate (pH 5.5–7.5) or 50 mM Tris (pH 7.5–9.0).

1-phosphate and 2-amino-6-mercapto-7-methyl purine [36]. The production of 2-amino-6-mercapto-7-methyl purine is monitored by following the increase in absorbance at 360 nm (ε_{360} = 10,000 M^{-1} cm^{-1}). Similarly, the PiPer assay (Life Technologies) continuously monitors phosphate levels by enzymatically converting maltose and inorganic phosphate to glucose and glucose-1-phosphate. The glucose is then oxidized to glucolactone and H_2O_2 by glucose oxidase, and the production of H_2O_2 is monitored using horseradish peroxidase, which converts H_2O_2 and Amplex Red into a fluorescent product, resorufin [37,38]. Although these assays are more sensitive than the AMP assay described in this article, they are limited in that they can be applied only to enzymes that form AMP through hydrolysis of ATP. As a result, they cannot be used to follow the activities of enzymes such as phosphodiesterases and ribonucleases, which do not release pyrophosphate as a product. In addition, because the production of inorganic phosphate is being monitored in these assays, they are incompatible with phosphate buffers.

The assay described here couples the deamination of AMP to the reduction of NAD^+. This allows the production of AMP to be monitored by measuring the change in absorbance at 340 nm. To our knowledge, this is the first time that the activity of AMP deaminase has been coupled to that of IMP dehydrogenase and the first time that NADH has been used as a readout for the production of AMP. This assay continuously monitors the production of AMP, allowing it to be used for both high-throughput drug screening and kinetic analyses. This has several advantages. First, the production of AMP is monitored in real time, simplifying the screening process. Second, because the assay can be used to monitor the time course of the reaction, both the binding affinity and mode of inhibition can be rapidly determined for any lead compound identified in the screen. Third, the assay described here is relatively inexpensive, requiring only readily available laboratory reagents and the production of two recombinant proteins. The simplicity of the assay makes it equally amenable for use in the research laboratory, high-throughput screening facilities, and high school and undergraduate classrooms. Lastly, whereas the assay described here can be used to accurately monitor AMP levels down to 5 μM, its sensitivity can be further increased by coupling the production of NADH to the bacterial luciferase-catalyzed oxidation of low-molecular-weight aldehydes [39–41]. Alternatively, the sensitivity of the assay can be increased by coupling it to the oxidation of NADH by resazurin, producing the red fluorescent resorufin product ($\varepsilon_{572}^{\text{resorufin}} = 73,000\ M^{-1}\ cm^{-1}$, λ_{em} = 585 nm, quantum yield = 0.74) [42].

In addition to monitoring enzymes that release AMP as their product, the assay can be used to monitor enzymes that can be coupled to the production of AMP via phosphodiesterases, ubiquitin and ubiquitin-like ligases, CoA ligases, aminoacyl–tRNA synthetases, or any other enzyme that releases AMP as a product. For example, ubiquitin and ubiquitin-like E_2 and E_3 ligases, as well as deubiquitinating enzymes, can be coupled to the AMP assay through the E_1 ligase, which releases AMP. The activity of adenylyl cyclases can be monitored by coupling the formation of cAMP by adenylyl cyclase to the hydrolysis of cAMP by PDE. Lastly, the reversible acetylation of histones, p53, and other proteins, which plays an essential role in gene regulation and protein function, can be monitored by coupling the protein acetylation and deacetylation reactions to acetyl–CoA synthetase, which releases AMP during the formation of acetyl–CoA. By coupling these pathways to the AMP assay, one can perform high-throughput kinetic analyses on each enzyme in the pathway. Specific steps in each pathway can be targeted by adjusting the enzyme concentrations such that the rate of the assay is dependent on the enzyme that catalyzes the targeted step. Alternatively, inhibitor screens can be designed to target all of the enzymes in the pathway simultaneously by adjusting the reaction conditions so that each step occurs at approximately the same rate.

Conclusion

We have developed a simple inexpensive assay to continuously monitor the production of AMP. This assay can be used to monitor the kinetics for enzymes that release AMP as a product as well as any enzyme in a pathway that can be coupled to a reaction that releases AMP. Applications include the high-throughput screening and characterization of lead compounds for potential drugs, including those used to treat pulmonary arterial hypertension, coronary heart disease, diabetes, dementia, depression, schizophrenia, cancer, and multidrug-resistant bacteria.

Disclosure statement

A provisional patent application based on the assays described in this article has been filed (U.S. Patent and Trademark Office application no. 62/060037).

Acknowledgments

The author acknowledges Kelly Tatchell for donation of the *S. cerevisiae* clones containing the open reading frames of IMP dehydrogenase and AMP deaminase and acknowledges James Cardelli and Floyd Galiano of the Feist–Weiller Cancer Center's Innovative North Louisiana Experimental Therapeutics (INLET) program for assistance and use of the Synergy 4 Hybrid Microplate Reader. This research was supported by funds from Louisiana State University Health Sciences Center in Shreveport and the Biomedical Research Foundation of Northwest Louisiana.

References

[1] E.A. Martis, R. Radhakrishnan, R.R. Badve, High-throughput screening: the hits and leads of drug discovery—an overview, J. Appl. Pharm. Sci. 1 (2011) 2–10.
[2] J. Austin, E.A. First, Catalysis of tyrosyl–adenylate formation by the human tyrosyl–tRNA synthetase, J. Biol. Chem. 277 (2002) 14812–14820.
[3] T.A. Kleeman, D. Wei, K.L. Simpson, E.A. First, Human tyrosyl–tRNA synthetase shares amino acid sequence homology with a putative cytokine, J. Biol. Chem. 272 (1997) 14420–14425.
[4] E. Gasteiger, A. Gattiker, C. Hoogland, I. Ivanyi, R.D. Appel, A. Bairoch, ExPASy: the proteomics server for in-depth protein knowledge and analysis, Nucleic Acids Res. 31 (2003) 3784–3788.
[5] L. Michaelis, M. Menten, Die Kinetik der Invertinwirkung, Biochem. Z. 49 (1913) 333–369.
[6] L. Michaelis, M.L. Menten, K.A. Johnson, R.S. Goody, The original Michaelis constant: translation of the 1913 Michaelis–Menten paper, Biochemistry 50 (2011) (1913) 8264–8269.
[7] G.A. Kohler, X. Gong, S. Bentink, S. Theiss, G.M. Pagani, N. Agabian, L. Hedstrom, The functional basis of mycophenolic acid resistance in *Candida albicans* IMP dehydrogenase, J. Biol. Chem. 280 (2005) 11295–11302.
[8] D.J. Merkler, A.S. Wali, J. Taylor, V.L. Schramm, AMP deaminase from yeast: role in AMP degradation, large scale purification, and properties of the native and proteolyzed enzyme, J. Biol. Chem. 264 (1989) 21422–21430.
[9] K. Murakami, AMP deaminase from baker's yeast: kinetic and molecular properties, J. Biochem. 86 (1979) 1331–1336.
[10] M. Yoshino, K. Murakami, K. Tsushima, AMP deaminase from baker's yeast: purification and some regulatory properties, Biochim. Biophys. Acta 570 (1979) 157–166.
[11] A.T. Bender, J.A. Beavo, Cyclic nucleotide phosphodiesterases: molecular regulation to clinical use, Pharmacol. Rev. 58 (2006) 488–520.
[12] Y.H. Jeon, Y.S. Heo, C.M. Kim, Y.L. Hyun, T.G. Lee, S. Ro, J.M. Cho, Phosphodiesterase: overview of protein structures, potential therapeutic applications, and recent progress in drug development, Cell. Mol. Life Sci. 62 (2005) 1198–1220.
[13] M.P. Kelly, N.J. Brandon, Differential function of phosphodiesterase families in the brain: gaining insights through the use of genetically modified animals, Prog. Brain Res. 179 (2009) 67–73.
[14] T. Keravis, C. Lugnier, Cyclic nucleotide phosphodiesterase (PDE) isozymes as targets of the intracellular signalling network: benefits of PDE inhibitors in

various diseases and perspectives for future therapeutic developments, Br. J. Pharmacol. 165 (2012) 1288–1305.
[15] A. Nishi, G.L. Snyder, Advanced research on dopamine signaling to develop drugs for the treatment of mental disorders: biochemical and behavioral profiles of phosphodiesterase inhibition in dopaminergic neurotransmission, J. Pharmacol. Sci. 114 (2010) 6–16.
[16] Y.J. Rao, L. Xi, Pivotal effects of phosphodiesterase inhibitors on myocyte contractility and viability in normal and ischemic hearts, Acta Pharmacol. Sin. 30 (2009) 1–24.
[17] M. Hochstrasser, Origin and function of ubiquitin-like proteins, Nature 458 (2009) 422–429.
[18] F. Ikeda, I. Dikic, Atypical ubiquitin chains: new molecular signals—"Protein Modifications: Beyond The Usual Suspects" review series, EMBO Rep. 9 (2008) 536–542.
[19] Y. Kimura, K. Tanaka, Regulatory mechanisms involved in the control of ubiquitin homeostasis, J. Biochem. 147 (2010) 793–798.
[20] J.J. Driscoll, E.S. Woodle, Targeting the ubiquitin + proteasome system in solid tumors, Semin. Hematol. 49 (2012) 277–283.
[21] M. Frezza, S. Schmitt, Q.P. Dou, Targeting the ubiquitin–proteasome pathway: an emerging concept in cancer therapy, Curr. Top. Med. Chem. 11 (2011) 2888–2905.
[22] L.N. Micel, J.J. Tentler, P.G. Smith, G.S. Eckhardt, Role of ubiquitin ligases and the proteasome in oncogenesis: novel targets for anticancer therapies, J. Clin. Oncol. 31 (2013) 1231–1238.
[23] M.D. Petroski, The ubiquitin system, disease, and drug discovery, BMC Biochem. 9 (Suppl. 1) (2008) S7.
[24] H.B. Kramer, B. Nicholson, B.M. Kessler, M. Altun, Detection of ubiquitin–proteasome enzymatic activities in cells: application of activity-based probes to inhibitor development, Biochim. Biophys. Acta 2012 (1823) 2029–2037.
[25] J.S. Schneekloth Jr., C.M. Crews, Natural product inhibitors of the ubiquitin–proteasome pathway, Curr. Drug Targets 12 (2011) 1581–1594.
[26] S. Singhal, M.C. Taylor, R.T. Baker, Deubiquitylating enzymes and disease, BMC Biochem. 9 (Suppl. 1) (2008) S3.
[27] B. Gadakh, A. Van Aerschot, Aminoacyl–tRNA synthetase inhibitors as antimicrobial agents: a patent review from 2006 till present, Expert Opin. Ther. Pat. 22 (2012) (2006) 1453–1465.
[28] G.H. Vondenhoff, A. Van Aerschot, Aminoacyl–tRNA synthetase inhibitors as potential antibiotics, Eur. J. Med. Chem. 46 (2011) 5227–5236.
[29] Z.P. Xiao, T.W. Ma, M.L. Liao, Y.T. Feng, X.C. Peng, J.L. Li, Z.P. Li, Y. Wu, Q. Luo, Y. Deng, X. Liang, H.L. Zhu, Tyrosyl–tRNA synthetase inhibitors as antibacterial agents: synthesis, molecular docking, and structure–activity relationship analysis of 3-aryl-4-arylaminofuran-2(5H)-ones, Eur. J. Med. Chem. 46 (2011) 4904–4914.
[30] K.G. Dyke, S.P. Curnock, M. Golding, W.C. Noble, Cloning of the gene conferring resistance to mupirocin in *Staphylococcus aureus*, FEMS Microbiol. Lett. 61 (1991) 195–198.
[31] F.L. Rock, W. Mao, A. Yaremchuk, M. Tukalo, T. Crepin, H. Zhou, Y.K. Zhang, V. Hernandez, T. Akama, S.J. Baker, J.J. Plattner, L. Shapiro, S.A. Martinis, S.J. Benkovic, S. Cusack, M.R. Alley, An antifungal agent inhibits an aminoacyl–tRNA synthetase by trapping tRNA in the editing site, Science 316 (2007) 1759–1761.
[32] Promega, Technical Manual: AMP–Glo Assay, Promega, Madison, WI, 2012.
[33] M. Staeben, K.M. Kleman-Leyer, A.L. Kopp, T.A. Westermeyer, R.G. Lowery, Development and validation of a Transcreener assay for detection of AMP- and GMP-producing enzymes, Assay Drug Dev. Technol. 8 (2010) 344–355.
[34] I. Cestari, K. Stuart, A spectrophotometric assay for quantitative measurement of aminoacyl–tRNA synthetase activity, J. Biomol. Screen. 18 (2013) 490–497.
[35] A.A. Baykov, O.A. Evtushenko, S.M. Avaeva, A malachite green procedure for orthophosphate determination and its use in alkaline phosphatase-based enzyme immunoassay, Anal. Biochem. 171 (1988) 266–270.
[36] A.J. Lloyd, H.U. Thomann, M. Ibba, D. Soll, A broadly applicable continuous spectrophotometric assay for measuring aminoacyl–tRNA synthetase activity, Nucleic Acids Res. 23 (1995) 2886–2892.
[37] M. Zhou, Z. Diwu, N. Panchuk-Voloshina, R.P. Haugland, A stable nonfluorescent derivative of resorufin for the fluorometric determination of trace hydrogen peroxide: applications in detecting the activity of phagocyte NADPH oxidase and other oxidases, Anal. Biochem. 253 (1997) 162–168.
[38] J.G. Mohanty, J.S. Jaffe, E.S. Schulman, D.G. Raible, A highly sensitive fluorescent micro-assay of H_2O_2 release from activated human leukocytes using a dihydroxyphenoxazine derivative, J. Immunol. Methods 202 (1997) 133–141.
[39] S.E. Brolin, E. Borglund, L. Tegner, G. Wettermark, Photokinetic micro assay based on dehydrogenase reactions and bacterial luciferase, Anal. Biochem. 42 (1971) 124–135.
[40] S. Golden, J. Katz, The determination of reduced nicotinamide adenine dinucleotide and metabolic intermediates in picomole amounts with bacterial luciferase, Biochem. J. 188 (1980) 799–805.
[41] P.E. Stanley, Determination of subpicomole levels of NADH and FMN using bacterial luciferase and the liquid scintillation spectrometer, Anal. Biochem. 39 (1971) 441–453.
[42] S. Barnes, J.G. Spenney, Stoichiometry of the NADH–oxidoreductase reaction for dehydrogenase determinations, Clin. Chim. Acta 107 (1980) 149–154.